SPC

Advanced Journal of Chemistry-Section A

Journal homepage: www.ajchem-a.com

Original Research Article

Synthesis, Solubility in Various Solvents, Spectroscopic Properties (FT–IR, ^{1}H, ^{13}C and ^{15}N–NMR, UV–Vis), NBO, NLO, FMO Analysis of A MNDPPD Drug

Mostafa Khajehzadeh*, **Mojtaba Baghernejad, Mehdi Rajabi, Sedigheh Rahmaniasl**

Young Researchers and Elite Club, Gachsaran Branch, Islamic Azad University, Gachsaran, Iran

ARTICLE INFO

Article history

Submitted: 01 November 2020
Revised: 03 December 2020
Accepted: 16 December 2020
Available online: 18 December 2020
Manuscript ID: AJCA-2011-1221

DOI: 10.22034/AJCA.2020.255373.1221

KEYWORDS

Spectroscopic properties
NLO
NBO
FMO analysis
Global hardness
Global softness
Electronegativity
Electrophilicity index
Solvent effect

ABSTRACT

In the present study, the complete structural and vibrational analysis of 3-methyle-4-(4-nitrophenyl)-4,8-dihydropyrazolo[4',3':5,6]pyrano[2,3-d]pyrimidine-5,7(1H,6H)-dione (**MNDPPD**) were evaluated using the theoretical and experimental methods. Then, the molecular structure of this drug optimized using the Gaussian 09 software with Hartree-Fock (**HF**) and density functional theory (**DFT**) methods with 6–311+G(d,2p) basis set. The ^{1}H and ^{13}C NMR spectra were computed using the gauge-invariant atomic orbital (GIAO) method, showing a good agreement with the experimental ones. The calculated vibrational frequencies and chemical shift values were compared using the FT-IR and NMR analysis. The last one UV–vis absorption spectra were analyzed at the presence of five solvent (H_2O, DMSO, CH_3CN, CH_3NO_2 and CH_3CHCl_2), saved at the range of 200–550 nm. The hyper-conjugative interaction energy and electron densities of donor and acceptor bonds were calculated using the natural bond orbital (NBO) analysis. In addition, frontier molecular orbitals analysis, non-linear optical (NLO) activity, electro negativity, ionization energy, global hardness, global softness, and the energy gap between the highest occupied molecular orbital (HOMO) to the lowest unoccupied molecular orbital (LUMO) were calculated. The results showed that the experimental and computational data are consistent with each other.

GRAPHICAL ABSTRACT

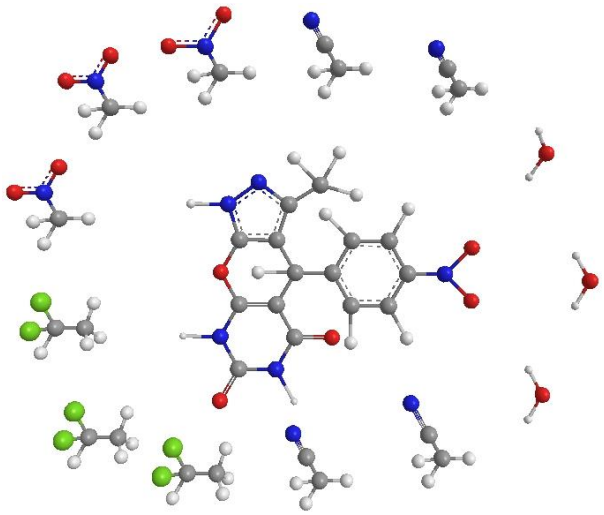

* Corresponding author: Khajehzadeh, Mostafa
✉ E-mail: khajehzadeh.chem@yahoo.com
☎ Tel number: +989177425331

Introduction

Chemical drugs have been widely used to treat various diseases. Nitrogenous heterocyclic compounds such as pyrazole, pyrazolone and its derivatives, have a special place in chemistry as they have an approved biological and pharmaceutical activities such as antimicrobial [1-9], antidiabetic [10], antioxidant [11], antitumor [12], antidepressant [13], Alzheimer's disease [14], Pyrazole is used to treat the inflammatory bowel syndrome [15], antipyretic [16], fungicides [17], pesticides [18] and herbicidal [19].

In recent years, many studies have been conducted to identify the therapeutic characteristics and molecular structure of drugs in laboratories. However, scientists are looking for ways to make their studies less costly and easier. One of the best methods for studying and simulating molecules in the gas phase is the use of computational methods and one of the best computational methods is the quantum mechanics method at various levels. Among the useful methods in quantum mechanics can be mentioned Hartree-Fock (HF**)** and density functional theory (DFT) [20]. This study calculated the molecular structure and spectroscopic properties on the MNDPPD antitumor drug using HF and B3LYP methods with 6-311+G(d,2p) basis set.

Scheme 1. Synthesis of MNDPPD antitumor drug

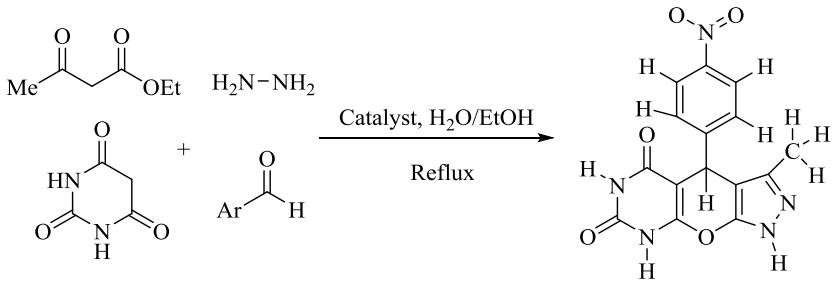

Experimental

All the chemicals with a purity of over 95% have been purchased from the Aldrich and Merck Chemical Company. The reaction progress was monitored by (TLC; silica-gel 60 F_{254}, n-hexane: Ethyl acetoacetate (4:1)). FT–IR spectra were recorded on 4000–400 cm^{-1} (KBr) with a FT–IR JASCO–680. The ^{1}H, ^{13}C–NMR spectra were obtained on a Bruker (DPX–400 MHz and 100 MHZ Avance 2 model) instrument DMSO-d_6 [21].

Synthesis of MNDPPD

Ethyl acetoacetate (1 mmol), hydrazine hydrate (1 mmol) and catalyst were added to H_2O/EtOH (5 mL, 50/50) over 20 min. Then, aldehyde (1 mmol) and barbituric acid (1 mmol) were added to the mixture and the mixture was heated under reflux. The reaction mixture was filtered and the resulting solid material was washed with EtOH (10 mL) in Soxhlet for 3 h and dried in a vacuum oven at 110 °C (Scheme 1) [21].

Computational Details

All the calculations were performed with Chem Bio Draw Ultra, Gaussian 09 [22], Gauss View 5.0 suite software. The calculations of the systems contain C, H, O and N described by the standard HF and B3LYP methods with 6–311+G(d,2p) basis set. At first, the drug structure was drawn up by Chem Bio Draw Ultra software and then optimized with Gaussian 09 software, and calculated the minimum energy, bond lengths and bond angles between the bonding atoms. The calculated stretching and bending harmonic vibrational frequencies for this drug by using these methods and the computational and experimental values were compared to each other [23]. The chemical shift values between protons, carbons and nitrogen were calculated by

using Chem Bio Draw Ultra and Gauge-invariant atomic orbital (GIAO) method and compared with experimental data [24]. Also, the non-linear optical (NLO) were used to calculate the polarizability and first hyper polarizability [25].

In addition, the natural bond orbital (NBO) were used to calculate the hybridization, global hardness, global softness, Mulliken charges, natural atomic charges, the type of electron transfer between the atoms, the energy difference between the highest occupied molecular orbital (HOMO) to the lowest unoccupied molecular orbital (LUMO) [26] and absorbed wavelengths were calculated by using UV–vis spectra and these methods in the presence of five solvent (H_2O, DMSO, CH_3CN, CH_3NO_2, and CH_3CHCl_2) [27].

Result and Discussion

Geometry optimization

Figure 1 depicts the MNDPPD antitumor and antibacterial drug studied in this work with atom numbering scheme which were optimized the Gaussian 09 software and DFT/B3LYP method with 6–311+G(d,2p) basis set. The most important bond lengths and bond angles of this drug in the gas phase are demonstrated in the Table 1. The results revealed that the C_{12}—C_{17} at the junction of two rings has the maximum bond length which were calculated with HF/6–311+G(d,2p)=1.531(Å), B3LYP=1.535 (Å) and C_{11}—C_{15}—C_{16} in the Pyrazole ring had the maximum bond angle which were calculated with HF/6–311+G(d,2p)=127.816° and B3LYP =128.180°. These calculated numbers depend on the position of the atoms in the bonds and they are valuable in their place [28].

Table 1. Optimized geometrical parameters of MNDPPD antitumor drug by **HF** and **DFT** (B3LYP) methods with 6-311+G(d,2p) basis set

Parameter	Methods		Parameter	Methods	
	HF	DFT (B3LYP)		HF	DFT (B3LYP)
Bond lengths (Å)	6-311+G(d,2p)	6-311+G(d,2p)	**Bond angles (°)**	6-311+G(d,2p)	6-311+G(d,2p)
N_1—C_2	1.366	1.380	C_2—N_1—C_6	127.261	127.757
C_2—N_3	1.375	1.394	N_1—C_2—N_3	113.392	112.655
C_2—O_7	1.186	1.210	N_1—C_2—O_7	124.110	124.770
C_4—C_5	1.338	1.357	N_3—C_2—O_7	122.495	122.572
C_4—O_9	1.339	1.363	C_2—N_3—C_4	123.212	123.500
C_5—C_{12}	1.524	1.526	N_3—C_4—C_5	123.646	123.373
C_6—O_8	1.191	1.217	N_3—C_4—O_9	110.730	110.984
C_{10}—C_{11}	1.347	1.367	C_5—C_4—O_9	125.621	125.637
C_{10}—N_{13}	1.327	1.345	C_4—O_9—C_{10}	113.791	112.896
C_{11}—C_{15}	1.429	1.426	O_9—C_{10}—C_{11}	127.646	127.875
C_{12}—C_{17}	1.531	1.535	O_9—C_{10}—N_{13}	122.544	122.830
N_{13}—N_{14}	1.346	1.362	C_{11}—C_{10}—N_{13}	109.807	109.284
N_{13}—H_{29}	0.898	1.004	C_{10}—C_{11}—C_{15}	102.764	103.440
C_{15}—N_{14}	1.297	1.330	C_5—C_{12}—C_{17}	112.202	111.632
C_{17}—C_{18}	1.387	1.397	C_{10}—N_{13}—N_{14}	110.116	110.491
C_{17}—C_{22}	1.391	1.399	C_{11}—C_{15}—C_{16}	127.816	128.180
C_{19}—C_{20}	1.379	1.390	C_{17}—C_{18}—C_{19}	120.925	120.891
C_{20}—C_{23}	1.464	1.477	C_{19}—C_{20}—N_{23}	119.116	119.167
N_{23}—O_{24}	1.188	1.225	C_{20}—N_{23}—O_{24}	117.617	117.665
N_{23}—O_{25}	1.187	1.224	O_{24}—N_{23}—O_{25}	124.701	124.598

Figure 1. Molecular structure of MNDPPD antitumor drug by **DFT**(B3LYP) method and 6-311+G(d,2p) basis set with atom numbering scheme

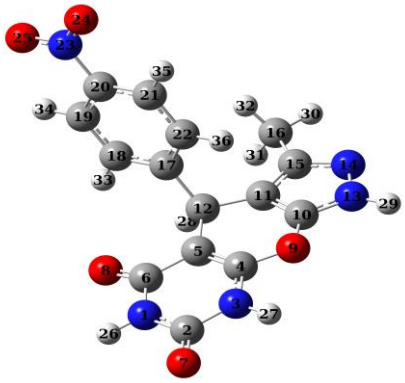

Vibrational assignments

The optimized molecular structure for the MNDPPD antitumor drug showed that the drug contains 36 atoms, molecular formula $C_{15}H_{11}N_5O_5$, symmetric point group **C1**, 102 normal vibrational modes, all of these vibrational modes are active in the FT–IR. Stretching and bending harmonic vibrational frequencies were ccalculated for this drug using the FT–IR JASCO-680 in laboratory conditions, and HF and B3LYP methods with 6-311+G(d,2p) basis set which are shown with (υ–stretching, π–in plane bending, α–out of plane bending). The computational data compared with experimental data and their spectrum (Figure 2 and 3). In addition, the computational frequencies are larger than experimental frequencies. Therefore, the scaling factor was used to correct the computational frequencies. Based on these calculations, the scaling factor (0.90) was used HF/6–311+G(d,2p) and scaling factor (0.96) was used B3LYP/6–311+G(d,2p) to correct the calculated frequencies [29].

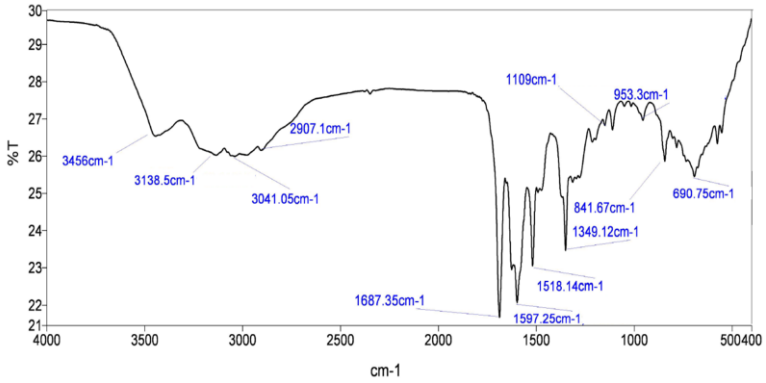

Figure 2. FT-IR spectra of MNDPPD antitumor drug by experimental method

The results revealed that the stretching frequency of the experimental spectrum was appeared in the range of 3456–1518 cm^{-1}, when computing with HF/6–311+G(d,2p) has appeared in the region 3526–1458 cm^{-1}, with B3LYP/6–311+G(d,2p) was appeared at the range of 3526–1490 cm^{-1}. Also, in plane bending frequency of the experimental spectrum has appeared in the region 1349–1109 cm^{-1}, when computing with HF/6–311+G(d,2p) has appeared in the region 1401–874 cm^{-1}, with B3LYP/6–311+G(d,2p) has appeared in the region 1338–1065 cm^{-1}. Also, out of plane bending frequency of the experimental spectrum has appeared in the region 953–690 cm^{-1}, when computing with HF/6–311+G(d,2p) has

appeared in the region 763–127 cm^{-1} , with B3LYP/6–311+G(d,2p) has appeared in the region 713–111 cm^{-1}.

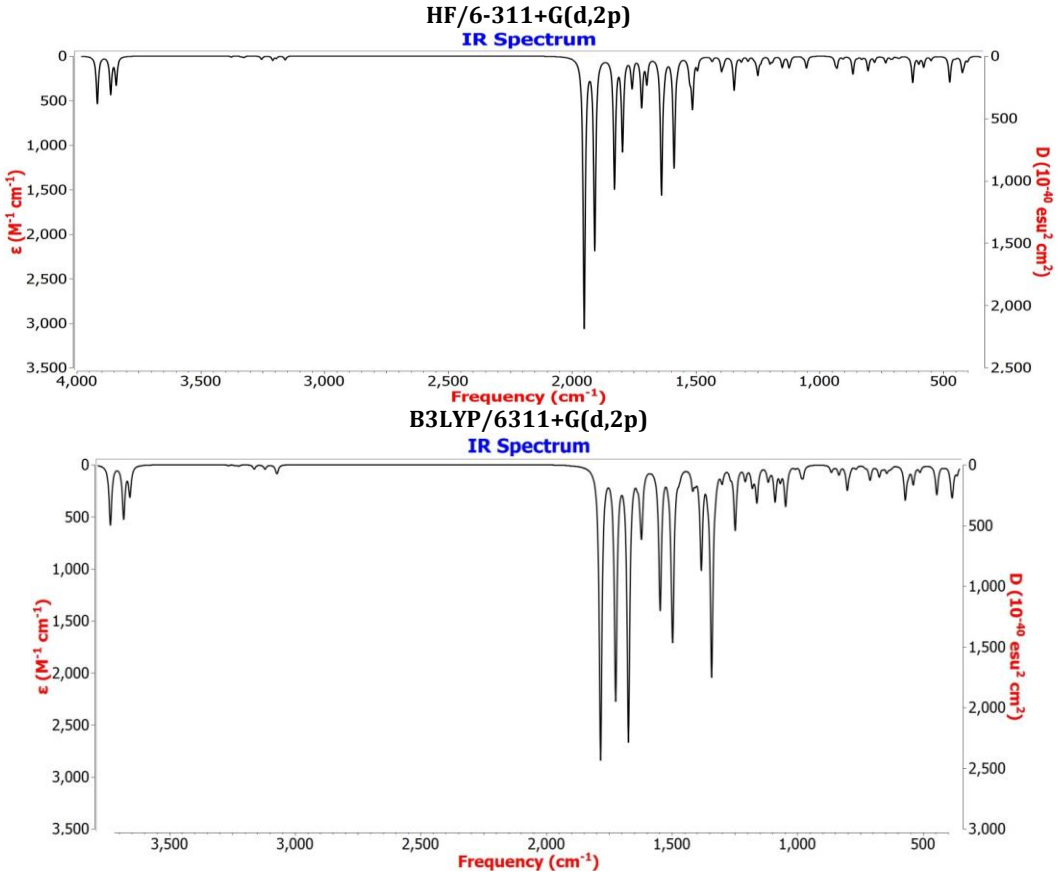

Figure 3. FT-IR spectra of MNDPPD antitumor drug by DFT/B3LYP and HF methods with 6-311+G(d,2p) basis sets

FT-IR spectral data for MNDPPD antitumor drug

Experimental

IR (KBr, cm^{-1}): υ=3456, 3138, 3041, 2907, 1678, 1597, 1518, 1349, 1109, 953, 841, 690.

HF/6–311+G(d,2p)

IR (cm^{-1}): υ=3526 (N_{13}—H_{29}), 3478 (N_3—H_{27}), 3458 (N_1—H_{26}), 2937 ($C_{16}H_{31}$), 1781 (C_2=O_7), 1743 (C_6=O_8), 1672 (C_4=C_5), 1643 (C_{19}—C_{20}), 1608 (C_{21}—C_{22}), 1556 (C_{10}—N_{13}), 1458 (C_{20}—N_{23}), π=1401 (N_1—H_{26}), 1281 (C_{18}—H_{33}), 1242 (C_{12}—H_{28}), 1106 (C_{19}—H_{34}), 1714 (N_3—H_{27}), 874 (C_{20}—N_{23}), α=763 (C_2=O_7), 739 (N_{23}—O_{25}), 700 (C_{22}—H_{36}), 603 (N_1—H_{25}), 470 (N_3—H_{27}), 425 (N_{13}—H_{29}), 127 (CH_3).

B3LYP/6–311+G(d,2p)

IR (cm^{-1}): υ=3526 (N_{13}—H_{29}), 3476 (N_3—H_{27}), 3453 (N_1—H_{26}), 3088 (C_{19}—H_{34}), 2993 ($C_{16}H_{31}$), 2952 ($C_{16}H_{32}$), 1711 (C_2=O_7), 1656 (C_6=O_8), 1608 (C_4=C_5), 1576 (C_{19}—C_{20}), 1564 (C_{21}—C_{22}), 1494 (C_{10}—N_{13}), 1490 (C_{20}—N_{23}), π=1338 (N_1—H_{26}), 1291 (C_{18}—H_{33}), 1285 (C_{12}—H_{28}), 1150 (C_{19}—H_{34}), 1141 (N_3—H_{27}), 1065 (C_{20}—N_{23}), α=713 (C_2=O_7), 679 (N_{23}—O_{25}), 636 (C_{22}—H_{36}), 583 (N_1—H_{25}), 466 (N_3—H_{27}), 408 (N_{13}—H_{29}), 111 (CH_3).

NMR spectrum analysis

^{1}H, ^{13}C and ^{15}N–NMR chemical shifts values of the MNDPPD antitumor drug were calculated experimentally in the laboratory using the Bruker (DPX–400 MHz and 100 MHZ Avance 2 model) instrument DMSO-d_6 (Figure 4). Also, the chemical shift values of protons, carbons and nitrogen were calculated by using Chem Bio Draw Ultra software, Gaussian 09W software with HF and B3LYP methods with 6–311+G(d,2p) basis set and gauge-invariant atomic orbital (GIAO) methods in the presence of five solvent (H_2O, DMSO, CH_3CN, CH_3NO_2 and CH_3CHCl_2) were used of the references **TMS B3LYP/6–311+G(2d,p) GIAO** and **NH3 B3LYP/6-311+G(2d,p) GIAO.** The computational and experimental values were compared with each other.

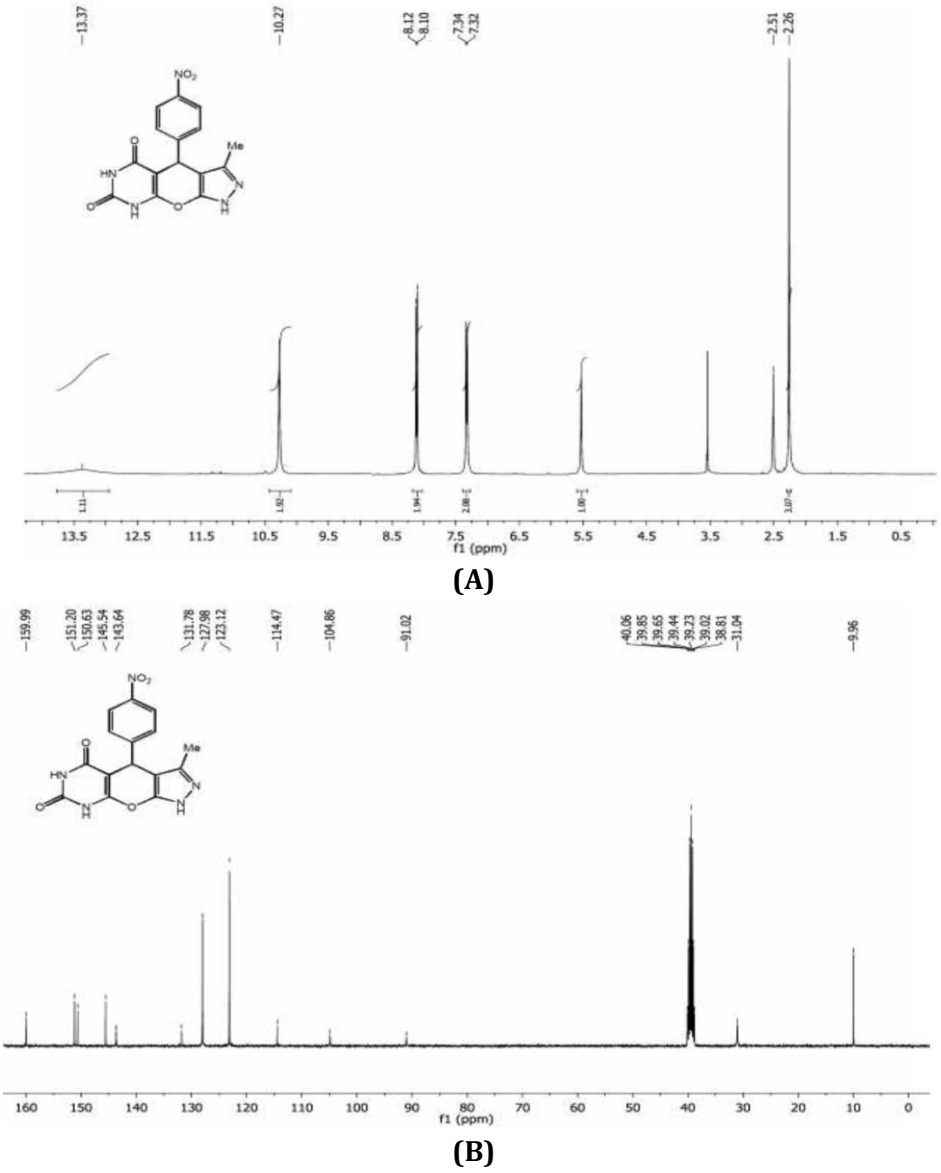

Figure 4. The calculated **(A)** ^{1}H, **(B)** ^{13}C NMR isotropic shifts (ppm) of MNDPPD antitumor drug by experimental method

Based on the results, chemical shift values of protons in the experimental method were calculated in the range of 13.37–2.26 ppm and Chem Bio Draw Ultra software in the area 12.57–1.93 ppm and HF/6–311+G(d,2p) in the range of 8.60–1.00 ppm and the B3LYP/6–311+G(d,2p) in the area 9.32–1.66 ppm. Also, chemical shift values of carbons in the experimental method were calculated in the range of 159.99–9.96 ppm, and Chem Bio Draw Ultra software in the range of 163.70–13.10 ppm, and HF/6–311+G(d,2p) in the range of 155.86–1.30 ppm and B3LYP/6–311+G(d,2p) in the range of 166.87–13.26 ppm. In addition, the chemical shift values of nitrogen were calculated by using HF/6–311+G(d,2p) in the range of 433–112 ppm and B3LYP/6–311+G(d,2p) in the range of 404–145 ppm [30].

^{1}H, ^{13}C–NMR spectral data for MNDPPD antitumor drug

Experimental

^{1}H NMR (**DMSO**-d_6, 400 MHz, δ ppm): 13.37 (br, 1H), 10.27 (s, 2H), 8.11 (d, 2H, *J*=8.0 Hz), 7.33 (d, 2H, *J*=8.0 Hz), 2.26 (s, 3H); ^{13}C NMR (**DMSO**-d_6, 100 MHz, δ ppm): 159.99 (CO), 159.90 (C), 151.20 (C), 150.63 (C), 145.54 (CO), 143.64 (C), 131.78 (CN), 127.98 (CH), 123.12 (CH), 114.47 (CH), 104.86 (CH), 91.02 (C), 39.85 (C), 31.04 (CH), 9.96 (CH_3).

Chem bio draw ultra

^{1}H NMR (*d* ppm): 12.57 (s, 1H), 10.98 (s, 1H), 10.81 (s, 1H), 8.17 (d, 2H), 7.70 (d, 2H), 4.74 (s, 1H), 1.93 (s, 3H); ^{13}C NMR (*d* ppm): 163.70 (d, 2CH) , 155.10 (C), 150.70 (CO), 148.40 (C), 144.90 (C), 139.10 (C), 129.90 (d, 2CH), 123.80 (d, 2CH), 113.40 (C), 81.30 (C), 34.90 (CH), 13.10 (CH_3).

HF/6-311+G(d,2p)

^{1}H NMR (**DMSO**, *d* ppm): 8.60 (s, 1H), 8.52 (s, 1H), 8.50 (s, 1H), 7.88 (s, 1H), 7.14 (s, 1H), 6.55 (s, 1H), 6.35 (s, 1H), 4.38 (s, 1H), 1.72 (s, 1H), 1.66 (s, 1H), 1.00 (s, 1H); ^{13}C NMR (**DMSO**, *d* ppm): 155.86 (CO), 150.55 (C), 146.42 (C), 144.79 (C), 140.43 (CO), 140.01 (C), 135.62 (CN), 122.78 (CH), 120.52 (CH), 120.26 (CH), 119.62 (CH), 83.13 (C), 75.82 (C), 17.54 (CH), 1.30 (CH_3); ^{15}N NMR (**DMSO**, *d* ppm): 433.61 (NO_2), 285.74 (N—N), 162.05, 142.25, 112.29 (C—N).

^{1}H NMR (**H_2O**, *d* ppm): 8.62 (s, 1H), 8.53 (s, 1H), 8.50 (s, 1H), 7.87 (s, 1H), 7.15 (s, 1H), 6.54 (s, 1H), 6.36 (s, 1H), 4.39 (s, 1H), 1.71 (s, 1H), 1.65 (s, 1H), 1.01 (s, 1H); ^{13}C NMR (**H_2O**, *d* ppm): 155.90 (CO), 150.59 (C), 146.46 (C), 144.81 (C), 140.46 (CO), 140.05 (C), 135.62 (CN), 122.76 (CH), 120.55 (CH), 120.26 (CH), 119.66 (CH), 83.12 (C), 75.81 (C), 17.53 (CH), 1.31 (CH_3); ^{15}N NMR (**H_2O**, *d* ppm): 433.67 (NO_2), 285.52 (N—N), 162.07, 142.29, 112.38 (C—N).

^{1}H NMR (**CH_3NO_2**, *d* ppm): 8.61 (s, 1H), 8.52 (s, 1H), 8.50 (s, 1H), 7.88 (s, 1H), 7.13 (s, 1H), 6.55 (s, 1H), 6.34 (s, 1H), 4.37 (s, 1H), 1.72 (s, 1H), 1.67 (s, 1H), 1.00 (s, 1H); ^{13}C NMR (**CH_3NO_2**, *d* ppm): 155.84 (CO), 150.52 (C), 146.39 (C), 144.78 (C), 140.41 (CO), 139.99 (C), 135.62 (CN), 122.79 (CH), 120.50 (CH), 120.25 (CH), 119.63 (CH), 83.13 (C), 75.82 (C), 17.54 (CH), 1.30 (CH_3); ^{15}N NMR (**CH_3NO_2**, *d* ppm): 433.56 (NO_2), 285.89 (N—N), 162.03, 142.23, 112.23 (C—N).

^{1}H NMR (**CH_3CN**, *d* ppm): 8.60 (s, 1H), 8.52 (s, 1H), 8.51 (s, 1H), 7.87 (s, 1H), 7.12 (s, 1H), 6.54 (s, 1H), 6.33 (s, 1H), 4.36 (s, 1H), 1.70 (s, 1H), 1.66 (s, 1H), 1.00 (s, 1H); ^{13}C NMR (**CH_3CN**, *d* ppm): 155.83 (CO), 150.51 (C), 146.38 (C), 144.77 (C), 140.40 (CO), 139.98 (C), 135.61 (CN), 122.78 (CH), 120.49 (CH), 120.25 (CH), 119.62 (CH), 83.11 (C), 75.81 (C), 17.52 (CH), 1.29 (CH_3); ^{15}N NMR (**CH_3CN**, *d* ppm): 433.52 (NO_2), 285.91 (N—N), 162.04, 142.22, 112.21 (C—N).

^{1}H NMR (**CH_3CHCl_2**, *d* ppm): 8.58 (s, 1H), 8.49 (s, 1H), 8.47 (s, 1H), 7.88 (s, 1H), 7.09 (s, 1H), 6.53 (s, 1H), 6.27 (s, 1H), 4.35 (s, 1H), 1.71 (s, 1H), 1.69 (s, 1H), 1.00 (s, 1H); ^{13}C NMR (**CH_3CHCl_2**, *d* ppm): 155.54 (CO), 150.17 (C), 146.10 (C), 144.65 (C), 140.18 (CO), 139.73 (C),

135.65 (CN), 122.89 (CH), 120.28 (CH), 120.19 (CH), 119.73 (CH), 83.15 (C), 75.87 (C), 17.55 (CH), 1.28 (CH_3); ^{15}N NMR (**CH_3CHCl_2**, *d* ppm): 433.06 (NO_2), 287.57 (N—N), 161.80, 141.98, 112.59 (C—N).

B3LYP/6-311+G(d,2p)

^{1}H NMR (**DMSO**, *d* ppm): 9.32 (s, 1H), 8.68 (d, 2H), 8.66 (s, 1H), 8.29 (s, 1H), 7.55 (s, 1H), 7.33 (s, 1H), 7.10 (s, 1H), 5.30 (s, 1H), 2.21 (s, 1H), 2.14 (s, 1H), 1.66 (s, 1H); ^{13}C NMR (**DMSO**, *d* ppm): 166.87 (CO), 160.57 (C), 159.53 (C), 154.08 (C), 153.89 (C), 153.00 (C), 151.35 (CO), 136.79 (C), 133.83 (CH), 128.88 (CH), 127.71 (CH), 103.31 (C), 97.29 (C), 39.05 (CH), 13.26 (CH_3); ^{15}N NMR (**DMSO**, *d* ppm): 405.14 (NO_2), 301.16 (N—N), 190.93, 177.38, 146.72 (C—N).

^{1}H NMR (**H_2O**, *d* ppm): 9.33 (s, 1H), 8.67 (d, 2H), 8.65 (s, 1H), 8.28 (s, 1H), 7.56 (s, 1H), 7.31 (s, 1H), 7.11 (s, 1H), 5.31 (s, 1H), 2.21 (s, 1H), 2.13 (s, 1H), 1.64 (s, 1H); ^{13}C NMR (**H_2O**, *d* ppm): 166.90 (CO), 160.61 (C), 159.57 (C), 154.09 (C), 153.89 (C), 153.04 (C), 151.38 (CO), 136.78 (C), 133.87 (CH), 128.89 (CH), 127.69 (CH), 103.32 (C), 97.28 (C), 39.02 (CH), 13.24 (CH_3); ^{15}N NMR (**H_2O**, *d* ppm): 405.20 (NO_2), 300.96 (N—N), 190.98, 177.40, 146.81 (C—N).

^{1}H NMR (**CH_3NO_2**, *d* ppm): 9.31 (s, 1H), 8.68 (d, 2H), 8.63 (s, 1H), 8.27 (s, 1H), 7.54 (s, 1H), 7.32 (s, 1H), 7.09 (s, 1H), 5.30 (s, 1H), 2.19 (s, 1H), 2.15 (s, 1H), 1.65 (s, 1H); ^{13}C NMR (**CH_3NO_2**, *d* ppm): 166.85 (CO), 160.53 (C), 159.51 (C), 154.07 (C), 153.89 (C), 152.98 (C), 151.33 (CO), 136.80 (C), 133.81 (CH), 128.87 (CH), 127.72 (CH), 103.31 (C), 97.28 (C), 39.05 (CH), 13.26 (CH_3); ^{15}N NMR (**CH_3NO_2**, *d* ppm): 405.11 (NO_2), 301.29 (N—N), 190.91, 177.36, 146.66 (C—N).

^{1}H NMR (**CH_3CN**, *d* ppm): 9.29 (s, 1H), 8.66 (d, 2H), 8.64 (s, 1H), 8.29 (s, 1H), 7.55 (s, 1H), 7.30 (s, 1H), 7.05 (s, 1H), 5.29 (s, 1H), 2.21 (s, 1H), 2.14 (s, 1H), 1.62 (s, 1H); ^{13}C NMR (**CH_3CN**, *d* ppm): 166.84 (CO), 160.50 (C), 159.49 (C), 154.03 (C), 153.86 (C), 152.97 (C), 151.32 (CO), 136.79 (C), 133.80 (CH), 128.85 (CH), 127.70 (CH), 103.29 (C), 97.26 (C), 39.03 (CH), 13.24 (CH_3); ^{15}N NMR (**CH_3CN**, *d* ppm): 405.10 (NO_2), 301.31 (N—N), 190.90, 177.36, 146.65 (C—N).

^{1}H NMR (**CH_3CHCl_2**, *d* ppm): 9.27 (s, 1H), 8.68 (d, 2H), 8.63 (s, 1H), 8.27 (s, 1H), 7.51 (s, 1H), 7.31 (s, 1H), 7.02 (s, 1H), 5.29 (s, 1H), 2.18 (s, 1H), 2.17 (s, 1H), 1.65 (s, 1H); ^{13}C NMR (**CH_3CHCl_2**, *d* ppm): 166.62 (CO), 160.17 (C), 159.23 (C), 154.02 (C), 153.88 (C), 152.73 (C), 151.10 (CO), 136.85 (C), 133.52 (CH), 128.79 (CH), 127.80 (CH), 103.30 (C), 97.23 (C), 39.04 (CH), 13.25 (CH_3); ^{15}N NMR (**CH_3CHCl_2**, *d* ppm): 404.68 (NO_2), 302.81 (N—N), 190.58, 177.16, 145.96 (C—N).

UV–vis spectrum analysis

The absorption spectrum of the MNDPPD antitumor drug exhibits features of three important wavelengths have been calculated which using **HF** method and 6–311+G(d,2p) basis set in the presence of DMSO, H_2O, CH_3CN, CH_3NO_2 and CH_3CHCl_2 solvents.

In addition, three important wavelengths were calculated using the **B3LYP** method and 6–311+G(d,2p) basis set in the presence of DMSO solvent with (λ_{max}=382.61, 340.43 and 322.94 nm), at the presence of the H_2O solvent with (λ_{max}=383.49, 340.83 and 323.51 nm), at the presence of CH_3NO_2 solvent with (λ_{max}=382.01, 339.90 and 322.53 nm), in the presence of CH_3CN solvent with (λ_{max}=381.94, 339.74 and 322.48 nm) and in the presence of CH_3CHCl_2 solvent with (λ_{max}=375.31, 335.24 and 318.64 nm). The most absorption for transfer from electron level of 88 → 89 was calculated (Figure 5) [31].

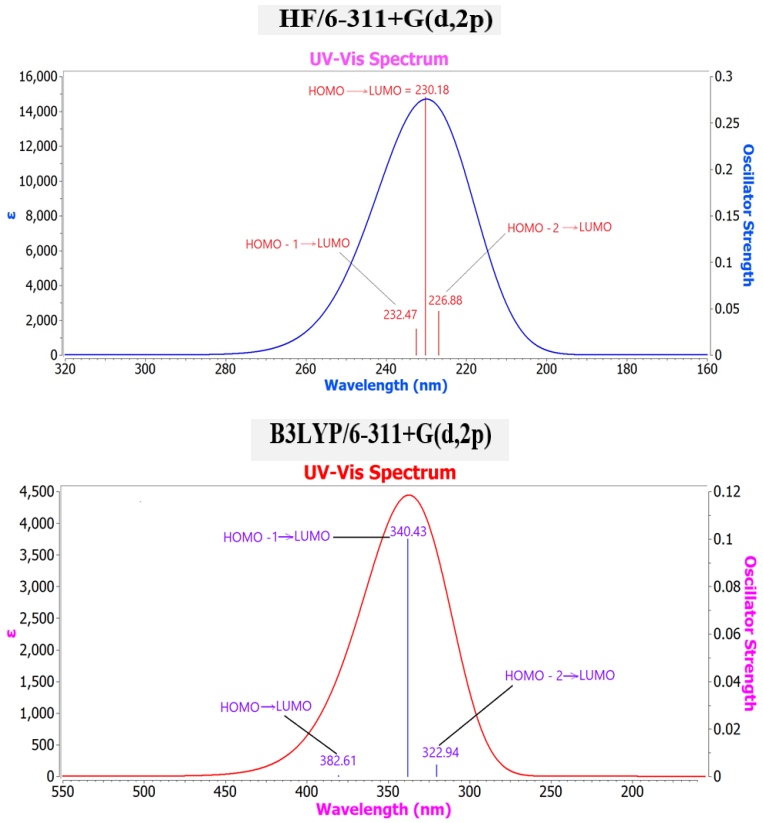

Figure 5. The UV–vis absorption spectrum in DMSO solvent of MNDPPD antitumor drug

Frontier molecular orbital (FMO) analysis

As seen in Table 2, the electro negativity (χ), ionization energy (I) (1), global hardness (η) (3), global softness (S) (4), electrophilicity index (ω) (6) and highest occupied molecular orbital (HOMO) and lowest unoccupied molecular orbital (LUMO) for MNDPPD antitumor drug were calculated using the HF/6–311+G(d,2p) and B3LYP/6–311+G(d,2p) at the presence of five solvent (DMSO, H_2O, CH_3CN, CH_3NO_2 and CH_3CHCl_2). The highest softness for this molecule was calculated by HF/6–311+G(d,2p) in the presence of a DMSO solvent is equal to 2.57745 eV, in the presence of a H_2O solvent is equal to 2.57864 eV, in the presence of CH_3CN solvent is equal to 2.57585 eV, in the presence of CH_3NO_2 solvent is equal to 2.57599 eV and in the presence of CH_3CN solvent is equal to 2.56370 eV. In addition, the highest softness for this molecule was calculated using the B3LYP/6–311+G(d,2p) in the presence of a DMSO solvent is equal to 7.26427 eV, in the presence of a H_2O solvent is equal to 7.27907 eV, in the presence of CH_3CN solvent is equal to 7.25268 eV, in the presence of CH_3NO_2 solvent is equal to 7.25373 eV and in the presence of CH_3CN solvent is equal to 7.13979 eV. This indicated that the molecule had a high polarization. Furthermore , the HOMO → LUMO was electron transfer from electron levels of 88 → 89. And $\Delta E_{HOMO-LUMO}$ is called energy gap. Also, electron transfers of HOMO–1 → LUMO and HOMO–2 → LUMO were calculated [32].

$$I = -E_{HOMO} \quad \text{(Eq. 1)}$$

$$A = -E_{LUMO} \quad \text{(Eq. 2)}$$

$$\eta = \frac{1}{2}(I - A) \quad \text{(Eq. 3)}$$

$$S = \frac{1}{2\eta} \quad \text{(Eq. 4)}$$

$$\chi = \frac{1}{2}(I + A) \quad \text{(Eq. 5)}$$

$$\omega = \frac{(-X)^2}{2\eta} \quad \text{(Eq. 6)}$$

Table 2. HOMO and LUMO energy value calculated by **HF** and **DFT** (B3LYP) methods with 6-311+G(d,2p) basis set for MNDPPD antitumor drug

Method	Solvents				
	DMSO	H_2O	CH_3CN	CH_3NO_2	CH_3CHCl_2
			HF		
E_{HOMO} (eV)	−0.34788	−0.34770	−0.34802	−0.34801	−0.34941
E_{LUMO} (eV)	0.04016	0.04010	0.04020	0.04020	0.04066
E_{HOMO-1} (eV)	−0.35317	−0.35302	−0.35329	−0.35328	−0.35444
E_{HOMO-2} (eV)	−0.36302	−0.36294	−0.36306	−0.36306	−0.36360
$\Delta E_{HOMO-LUMO\ gap}$ (eV)	0.38804	0.38780	0.38822	0.38821	0.39007
I (eV)	0.34788	0.34770	0.34802	0.34801	0.34941
A (eV)	−0.04016	−0.04010	−0.04020	−0.04020	−0.04066
η (eV)	0.19399	0.19390	0.19411	0.19410	0.19503
S (eV)	2.57745	2.57864	2.57585	2.57599	2.56370
χ (eV)	0.15386	0.15380	0.15391	0.15367	0.15437
ω (eV)	0.06099	0.06095	0.06101	0.06083	0.06109
			DFT		
E_{HOMO} (eV)	−0.24970	−0.24952	−0.24983	−0.24982	−0.25122
E_{LUMO} (eV)	−0.11203	−0.11213	−0.11195	−0.11196	−0.11116
E_{HOMO-1} (eV)	−0.26348	−0.26332	−0.26361	−0.26360	−0.26484
E_{HOMO-2} (eV)	−0.26996	−0.26950	−0.26978	−0.26977	−0.27104
$\Delta E_{HOMO-LUMO\ gap}$ (eV)	0.13767	0.13739	0.13788	0.13786	0.14006
I (eV)	0.24970	0.24952	0.24983	0.24982	0.25122
A (eV)	0.11203	0.11213	0.11195	0.11196	0.11116
η (eV)	0.06883	0.06869	0.06894	0.06893	0.07003
S (eV)	7.26427	7.27907	7.25268	7.25373	7.13979
χ (eV)	0.18086	0.18082	0.18089	0.18089	0.18119
ω (eV)	0.23761	0.23795	0.23817	0.23817	0.23439

HOMO → LUMO (88 → 89), global hardness (η), global softness (S), electrophilicity index (ω), electro negativity (χ)

Natural bond orbital (NBO) analysis

Natural bond orbital analysis (NBO) is an important method to determine the electric charge of the atoms, hybridization and natural electron configuration in orbitals **s**, **p**, **d** and **f** [33]. The NBO data for the occupancies and hybridization of C—N, C═O, N—O, N—H and N—N bonds are presented in Table 3. According to the NBO result, the **C** atom forms a sigma bond with N and the σ(C—N) bond is formed from an $sp^{1.08}$ hybrid on C (which is a mixture of 32.71% s, 35.64% p, and 0.11% d AO) and $sp^{0.95}$ hybrid on N (wich is a mixture of 67.19% s, 64.31% p, and 0.05% d AO). One the other hand, the π(C═O) bond was formed from an $sp^{2.48}$ hybrid on C (wich is a mixture of 0.04% s, 99.44% p, and 0.52% d AO) and $sp^{1.99}$ hybrid on O (wich is a mixture of 0.05% s, 99.84% p, and 0.12% d AO). NBO analysis can show us occupancy and the interaction between the bonding atoms and showing the electron transfer between the atoms which are electron donor and electron acceptor [34]. NBO analysis for MNDPPD antitumor drug were calculated by HF/6–311+G(d,2p) and B3LYP/6–311+G(d,2p) in the presence of DMSO solvent Table 4. Results include information such as acceptor (j), donor (i), type, $\varepsilon_{(i)} - \varepsilon_{(j)}{}^{b}$, occupancy, $E^{(2)}$, $F_{(i,\ j)}{}^{c}$ that $E^{(2)}$ was calculated using the Equation 7.

$$E^{(2)}=\Delta E_{ij} = q_i \frac{F(i,j)^2}{\varepsilon_i - \varepsilon_j} \qquad \text{(Eq. 7)}$$

Where q_i is the value of donor orbital, ε_i and ε_j are diagonal elements, $F_{(i,j)}$ is the off- diagonal NBO Fock matrix element. Whatever the value of $E^{(2)}$ is more, it indicates that the interaction between the atoms is more. Based on the results, most electron transfer is of the type π → π^*, which were calculated with HF/6–311+G(d,2p), between π(C_{17}—C_{18}) → π^*(C_{19}—C_{20}) with $E^{(2)}$= 56.39 kcal/mol and with B3LYP/6-311+G(d,2p), between π(C_{19}—C_{20}) → π^*(N_{23}—O_{25}) with $E^{(2)}$= 28.86 kcal/mol.

Table 3. The NBO Results for occupancies and hybridization of C—N, C═O, N—O, N—H and N—N bonds

B3LYP/6-311+G(d,2p)		[AO]%								
NBO	**Occupancy**	**% *s***		**% *p***		**% *d***		**S. P. $C_{(A-B)}$%**		**Hybridation**
(A—B) bond		A	B	A	B	A	B	A	B	
σ (C_2—N_1)	1.98	32.71	67.19	35.64	64.31	0.11	0.05	38.02	61.98	$0.61(sp^{1.08})$C+ $0.78(sp^{0.95})$N
π (C_2═O_7)	1.99	0.04	0.05	99.44	99.84	0.52	0.12	27.57	72.43	$0.52(sp^{2.48})$C+ $0.85(sp^{1.99})$O
σ (N_{23}—O_7)	1.99	31.73	25.13	68.13	74.73	0.13	0.14	48.87	51.13	$0.69(sp^{2.14})$N+ $0.71(sp^{2.97})$O
σ (N_1—H_{26})	1.98	27.68	99.91	72.28	0.09	0.04	0.00	72.11	27.89	$0.84(sp^{2.16})$N+ $0.52(s^{9.00})$H
σ (N_{13}—N_{14})	1.98	30.47	21.36	69.46	78.48	0.07	0.15	55.07	44.93	$0.74(sp^{2.27})$N+ $0.67(sp^{3.67})$N

S. P. C: Square of polarization co-efficients

Table 4. Second order perturbation theory of Fock matrix in NBO Basis for MNDPPD antitumor drug by **HF** and **DFT** (B3LYP) methods with 6-311+G(d,2p) basis set

			HF			
Donor(i)	**Types**	**Acceptor(j)**	**Types**	$E(2)^a$	**E(i)–$E(j)^b$**	$F(i,j)^c$
C_4—C_5	π	C_6—O_8	π^*	37.43	0.60	0.13
C_{10}—C_{11}	π	N_{14}—C_{15}	π^*	50.41	0.55	0.15
C_{17}—C_{18}	π	C_{19}—C_{20}	π^*	56.39	0.46	0.14
C_{17}—C_{18}	π	C_{21}—C_{22}	π^*	34.68	0.49	0.11
C_{19}—C_{20}	π	N_{23}—O_{25}	π^*	34.91	0.33	0.10
LP(1)N_1		C_2—O_7	π^*	66.61	0.63	0.18
LP(1)N_1		C_6—O_8	π^*	68.60	0.60	0.18
LP(1)N_3		C_2—O_7	π^*	62.29	0.65	0.17
LP(1)N_3		C_4—C_5	π^*	64.37	0.60	0.17
LP(2)O_9		C_4—C_5	π^*	44.21	0.73	0.16
LP(1)N_{13}		C_{10}—C_{11}	π^*	86.92	0.55	0.19
LP(1)N_{13}		N_{14}—C_{15}	π^*	41.69	0.55	0.13

DFT (B3LYP)						
Donor(i)	**Types**	**Acceptor(j)**	**Types**	$E(2)^a$	**E(i)-$E(j)^b$**	$F(i,j)^c$
C_4—C_5	π	C_6—O_8	π^*	24.49	0.31	0.08
C_{10}—C_{11}	π	N_{14}—C_{15}	π^*	27.04	0.29	0.08
C_{17}—C_{18}	π	C_{19}—C_{20}	π^*	25.05	0.27	0.07
C_{17}—C_{18}	π	C_{21}—C_{22}	π^*	18.14	0.28	0.06
C_{19}—C_{20}	π	N_{23}—O_{25}	π^*	28.86	0.13	0.05
LP(1)N_1		C_2—O_7	π^*	61.08	0.27	0.11
LP(1)N_1		C_6—O_8	π^*	50.41	0.28	0.10
LP(1)N_3		C_2—O_7	π^*	53.51	0.28	0.11
LP(1)N_3		C_4—C_5	π^*	46.11	0.30	0.10
LP(2)O_9		C_4—C_5	π^*	30.77	0.37	0.09
LP(1)N_{13}		C_{10}—C_{11}	π^*	46.31	0.29	0.10
LP(1)N_{13}		N_{14}—C_{15}	π^*	25.36	0.29	0.07

[a]E^2=means energy of hyper conjugative interaction (stabilization energy), [b]Energy difference between donor and acceptor i and j NBO orbitals. [c]F(i, j) is the Fock matrix element between i and j NBO orbitals

Hyperpolarizability calculations

Non-linear optical (NLO) activity arises from frequency shifting, optical interconnections, optical memory and optical switching [35].

Total dipole moment (μ_{total}), the first order hyperpolarizability (β_{total}), linear polarizability (α) and (Δα) were calculated using the following formula for MNDPD antitumor drug were calculated by using Gaussian 09 software with HF/6–311+G(d,2p) and B3LYP/6–311+G(d,2p). Table 5.

$\beta_x = \beta_{xxx} + \beta_{xyy} + \beta_{xzz}$ (Eq. 8)

$\beta_y = \beta_{yyy} + \beta_{xxy} + \beta_{yzz}$ (Eq. 9)

$\beta_z = \beta_{zzz} + \beta_{xxz} + \beta_{yyz}$ (Eq. 10)

$$\beta_{total} = \sqrt{(\beta^2_x + \beta^2_y + \beta^2_z)} \quad \text{(Eq. 11)}$$

$$\mu = \sqrt{(\mu^2_x + \mu^2_y + \mu^2_z)} \quad \text{(Eq. 12)}$$

$$\alpha_{total} = \frac{(\alpha xx + \alpha yy + \alpha zz)}{3} \quad \text{(Eq. 13)}$$

$$\Delta\alpha = \sqrt{((\alpha xx - \alpha yy)^2 + (\alpha yy - \alpha zz)^2 + (\alpha zz - \alpha xx)^2/2)} \quad \text{(Eq. 14)}$$

Based on calculated results, the most μ_{total}=8.764 Debye, the most α_{total}= –161.912, the most Δα=36.088 and β_{total}=285.730

Natural population analysis

The natural atomic charges played an important role in determining the vibrational properties, the state of electrons on the atoms in the Lewis structure, positive and negative charge of atoms, dipole moment, polarizability, formation of the bond between atoms for MNDPPD antitumor drug [36].

In this research study, the Mulliken charges and natural atomic charges distribution of the molecule were calculated on HF and B3LYP levels with 6–311+G(d,2p) basis set. The illustration of Mulliken and natural charge plot is depcted in Figure 6, respectively. The nitrogen atoms are N_1, N_3, N_{13} and N_{14} negative charge. However, the N_{23} have a positive charge. This was due to the structure of NO_2, oxygen atoms that have more electro negativity. So it absorbs nitrogen electron. In addition, there were five oxygen atoms in the molecular structure this drug and all of them have a negative charge. Also, C_2 and C_6

atoms which are present in the carboxyl group have a positive charge. In addition, all the hydrogen atoms have a positive charge [37].

Table 5. The electronic dipole moment (μ) (Debye), polarizability (α) and first hyper polarizability (β) of MNDPPD antitumor drug by **HF** and **DFT** (B3LYP) methods with 6-311+G(d,2p) basis set

parameter	HF a.u.	B3LYP a.u.
μ_x	−7.528	−7.598
μ_y	4.243	4.297
μ_z	−0.492	−0.775
μ_{total}	8.655	8.764
α_{xx}	−181.296	−180.244
α_{xy}	−4.356	−4.481
α_{yy}	−164.562	−162.948
α_{xz}	13.291	13.903
α_{yz}	−2.984	−3.679
α_{zz}	−139.878	−139.881
α_{total}	−161.912	−161.034
$\Delta\alpha$	36.088	35.074
β_{xxx}	−265.550	−268.349
β_{xyy}	39.786	38.268
β_{xzz}	−21.748	−24.129
β_{yyy}	−42.189	−38.970
β_{xxy}	145.729	141.220
β_{yzz}	24.874	26.544
β_{zzz}	−15.172	−18.318
β_{yyz}	7.162	5.525
β_{xxz}	36.580	33.548
β_{total}	280.301	285.730

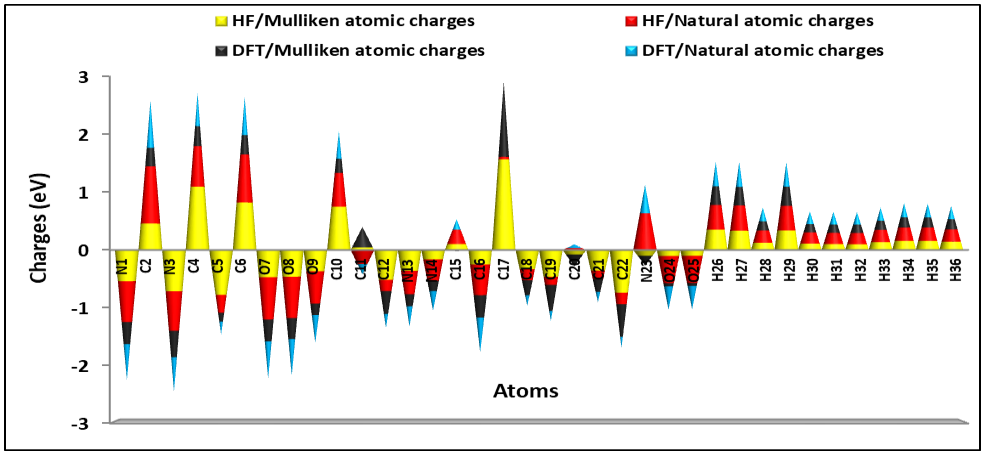

Figure 6. Mulliken charge and natural atomic charges distribution of MNDPPD antitumor drug by **HF** and **B3LYP** methods with 6-311+G(d,2p) basis set

In this study, molecular electrostatic potential counter map (MESP) constricted by HF/6–311+G(d,2p) and B3LYP/6–311+G(d,2p) method using Gauss View 5.0 program. (MESP) correlates with electro negativity (χ), dipole moment (μ) and site of chemical reactivity of the molecule

Fig. 7. In the molecular structure of this drug, the negative regions are mainly localized on the oxygen and nitrogen atoms, N_1, N_3, N_{13}, N_{14} and O_7, O_8, O_9, O_{24}, O_{25} atoms. Molecular electrostatic potential counter map shows that the negative potential site on electronegative atoms (N and O) as well as the positive potential site is around the hydrogen atom.

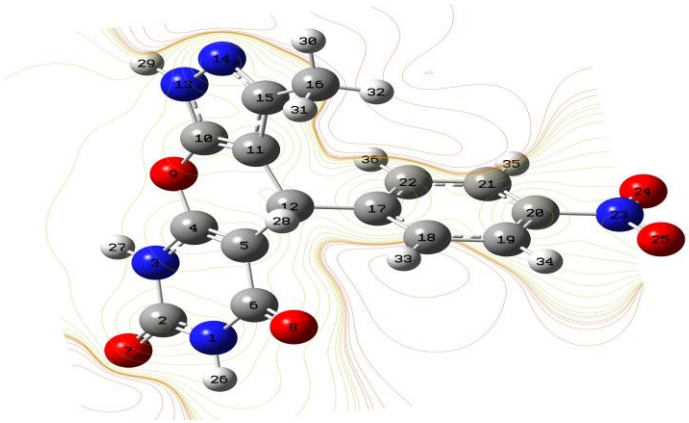

Figure 7. Molecular electrostatic potential (MESP) in gas phase of MNDPPD antitumor drug by **HF** and **B3LYP** methods with 6-311+G(d,2p) basis set

Conclusion

Pyrazole, pyrazolone and its derivatives, have a special place in chemistry as they have biological, pharmaceutical, and therapeutic activities. In this work, the molecular structure of the MNDPPD antitumor drug was analyzed. First, the stretching and bending harmonic vibrational frequencies were ccalculated using the FT–IR experimental spectrum and HF and B3LYP methods with 6–311+G(d,2p) basis set. ^{1}H, ^{13}C and ^{15}N–NMR chemical shifts values were determined using the experimental and computational spectra in the presence of DMSO solvent. Electro negativity (χ), ionization energy (I), global hardness (η), global softness (S), electrophilicity index (ω), HOMO and LUMO were calculated by using FMO analysis. Also, NBO were used for determining the charge of atoms, hybridization, natural electron configuration in orbitals, occupancies, hybridization and natural atomic charges. The highest softness for this molecule was calculated by HF/6–311+G(d,2p) in the presence of a DMSO solvent is equal to 2.57745 eV, and the highest softness for this molecule was calculated using the B3LYP/6–311+G(d,2p) in the presence of a DMSO solvent is equal to 7.26427 eV. These results show that the molecule has a lot of softness and the softer the molecule, the greater its polarity.

Acknowledgement

The support from Young Researchers and Elite Club of Islamic Azad University of Gachsaran is thankfully acknowledged.

Disclosure statement

No potential conflict of interest was reported by the authors.

ORCID

Mostafa Khajehzadeh: 0000-0002-3814-9021

References

[1] A. Tanitame, Y. Oyamada, K. Ofuji, H. Terauchi, M. Kawasaki, M. Wachi, J. Yamagishi, *Bioorg. Med. Chem. Lett.*, **2005**, *15*, 4299–4303.

[2] N. Manju, B. Kalluraya, S. Kumar, B. Revanasiddappa, *J. Med. Chem. Sci.*, **2019**, *2*, 101–109.

[3] S. Sadegh-Malvajerd, Z. Arzehgar, F. Nikpour, *Z. Naturforsch. B*, **2013**, *68*, 182–186.
[4] Z. Arzehgar, H. Ahmadi, *J. Chinese Chem. Soc*., **2019**, *66*, 303–306.
[5] Z. Moghadasi, *J. Med. Chem. Sci*., **2019**, *2*, 35–37.
[6] G. Feng, S. Xu, R. Chen, W. Chen, K.K. Wang, S. Wang, *Tetrahedron Lett*., **2020**, *61*, 152622.
[7] G. Cao, X. Liu, L. Wang, Y. Li, D. Teng, *Tetrahedron Lett*., **2020**, *76*, 131568.
[8] P.B. Schettino, C. Bustos, E. Molins, X. Figueroa, J. Llanquinao, X. Zarate, G. Vallejos, C. Diaz-Uribe, W. Vallejo, E. Schott, *Arab. J. Chem.*, **2020**, *13*, 6412–6424.
[9] S. Punia, V. Verma, D. Kumar, A. Kumar, L. Deswal, *J. Mol. Struct*., **2021**, *1223*, 129216.
[10] K.R.A. Abdellatif, M.A. Chowdhury, *Bioorg. Med. Chem*., **2009**, *17*, 5182–5188.
[11] D.M. Shen, E.J. Brady, M.R. Candelore, Q. Dallas-Yang, V.D.H. Ding, W.P. Feeney, G. Jiang, M.E. McCann, S. Mock, S.A. Qureshi, R. Saperstein, *Bioorg. Med. Chem. Lett*., **2011**, *21*, 76–81**.**
[12] J.S. Casas, E.E. Castellano, J. Ellena, M.S. García-Tasende, M.L. Perez-Paralle, A. Sánchez, , Á. Sánchez-González, , J. Sordo, Á. Touceda,*., J. Inorg. Biochem*., **2008**, *102*, 33–45.
[13] L. Bhat, B. Jandeleit, T.M. Dias, T.L. Moors, M.A. Gallop, *Bioorg. Med. Chem. Lett*., **2005**, *15*, 85–87.
[14] M. Chioua, A. Samadi, E. Soriano, O. Lozach, L. Meijer, M. Contelles, *J. Bioorg. Med. Chem. Lett*., **2009**, *19*, 4566–4569.
[15] P. Lan, Z.J. Huang, J.R. Sun, W.M. Chen, *Int. J. Mol. Sci*., **2010**, *11*, 3357–3374.
[16] L.C. Behr, R. Fusco, C.H. Jarboe, A. Weissberger, *The Chemistry of Heterocyclic Compounds*, Interscience: New York, **1967**.
[17] D. Singh, *J. Indian Chem. Soc*., **1991**, *68*, 165–167.
[18] M. Londershausen, *Pestic. Sci*., **1996**, *48*, 269–292.
[19] C.B. Vicentini, S. Guccione, L. Giurato, R. Ciaccio, D. Mares, G.J. Forlani, *Agric. Food Chem*., **2005**, *53*, 3848–3855.
[20] D.R. Leenaraj, D. Manimaran, I.H. Joe, *J. Mol. Struct*., **2016**, *1123*, 180–190.
[21] S. Dastkhoon, Z. Tavakoli, S. Khodabakhshi, M. Baghernejad, M. Khaleghi, *New. J. Chem*., **2015**, *39*, 7268–7271.
[22] M.J. Frisch, G.W. Trucks, H.B. Schlegel, G.E. Scuseria, M.A. Robb, J.R. Cheeseman, G. Scalmani, V. Barone, B. Mennucci, G. Petersson, H. Nakatsuji, *Gaussian, Inc*., *Wallingford CT*, **2009**.
[23] M. Khajehzadeh, M. Moghadam, *Spectrochim. Acta Part A. Mol. Biomol. Spectrosc*., **2017**, *180*, 51–66.
[24] M. Khajehzadeh, N. Sadeghi, *J. Mol. Liq*., **2018**, *249*, 281–293.
[25] M. Khajehzadeh, N. Sadeghi, *J. Mol. Liq*., **2018**, *256*, 238–246.
[26] M. Khajehzadeh, M. Rajabi, S. Rahmaniasl, *J. Mol. Struct*., **2019**, *1175*, 139–151.
[27] G. Halil, Ö. Nuri, C. Ümit, A.Y. Bingöl, A. Gökhan, *Mol. Biomol. Spectros*., **2016**, *163*, 170–180.
[28] A. Nataraj, V. Balachandran, T. Karthick, *J. Mol. Struct*., **2012**, *1022*, 94–108.
[29] G. Ramachandran, S. Muthu, S. Renuga, *Spectrochim. Acta Part A*., **2013**, *107*, 386–398.
[30] B. Amul, S. Muthu, M. Raja, S. Sevvanthi, *J. Mol. Struct*., **2019**, *1195*, 747–761.
[31] A.M. Fahim, M.A. Shalaby, M.A. Ibrahim, *J. Mol. Struct*., **2019**, *1194*, 211–226.
[32] S. Samiee, P. Hossienpour, *Inorg. Chimi. Acta*., **2019**, *494*, 13–20.
[33] I.V. Mirzaeva, N.K. Moroz, I.V. Andrienko, E.A. Kovalenko, *J. Mol. Struct*., **2018**, *1163*, 68–76.
[34] K. Sharma, R. Melavanki, S.S. Patil, R. Kusanur, N.R. Patil, V.M. Shelar, *J. Mol. Struct*., **2019**, *1181*, 474–487.
[35] D.A. Zainuri, S. Arshad, N.C. Khalib, I.A. Razak, *J. Mol. Struct*., **2017**, *1128*, 520–533.

[36] M.D. Mohammadi. M. Hamzehloo, *Comput. Theo. Chem*., **2018**, *1144*, 26–37.

[37] S. Bhunia, A. Kumar, A. Singh, A.K. Ojha, *Comput. Theo. Chem*., **2018**, *1141*, 7–14.

HOW TO CITE THIS ARTICLE

Mostafa Khajehzadeh*, Mojtaba Baghernejad, Mehdi Rajabi, Sedighrh Rahmaniasl. Synthesis, Solubility in Various Solvents, Spectroscopic Properties (FT–IR, ^{1}H, ^{13}C and ^{15}N–NMR, UV–Vis), NBO, NLO, FMO Analysis of A MNDPPD Drug. *Adv. J. Chem. A*, 2021, 4(1), 42-57.

DOI: 10.22034/AJCA.2020.255373.1221
URL: http://www.ajchem-a.com/article_120600.html